Metal Radical Complexes

DOI: 10.1002/anie.200701194

The Geometric and Electronic Structure of a One-Electron-Oxidized Nickel(II) Bis(salicylidene)diamine Complex**

*Tim Storr, Erik C. Wasinger, Russell C. Pratt, and T. Daniel P. Stack**

The cooperativity of transition-metal ions and proradical ligands in metalloenzyme active sites is of current research interest.[1] In an effort to understand the intricacies of the interaction of metal ions with organic radicals, many transition-metal complexes with one or more organic radical ligands have been studied.[2–4] Depending on the relative energies of the redox-active orbitals, metal complexes with proradical ligands can exist in a limiting description as a metal–ligand-radical ($M^{n+}(L^{\bullet})$) or a high-valent metal complex ($M^{(n+1)+}(L^{-})$). Given favorable energetics, valence tautomerism can occur through variation of the ligand field or temperature.[2,5–9] In particular, much recent interest exists in nickel(II) bis(salicylidene)diamine complexes (Scheme 1),[6–10] as the one-electron-oxidized forms $\mathbf{1}^+$, $\mathbf{2}^+$, and $\mathbf{3}^+$ have been reported to exhibit temperature-dependent valence tautomerism between $Ni^{II}(L^{\bullet-})$ and $Ni^{III}(L^{2-})$ forms.

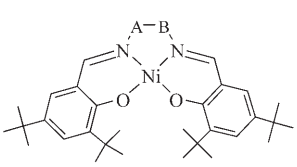

1, A–B=*rac*-1,2-cyclohexanediyl
2, A=B=CH_2

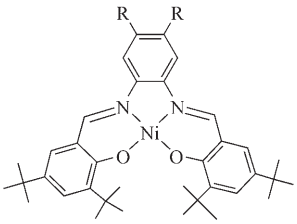

3, R=H
4, R=Me

Scheme 1. Nickel(II) bis(salicylidene)diamine complexes.

[*] Dr. T. Storr, Dr. R. C. Pratt, Prof. T. D. P. Stack
Department of Chemistry
Stanford University
Stanford, CA 94305 (USA)
Fax: (+1) 650-725-0259
E-mail: stack@stanford.edu
Dr. E. C. Wasinger[+]
California State University, Chico
Chico, CA (USA)

[+] Current Address:
Argonne National Laboratory
Argonne, IL (USA)

[**] This work was supported by an NIH grant (GM-50730), and an NSERC postdoctoral fellowship (T.S.). SSRL operations are funded by the DOE, Office of Basic Energy Services. We thank Prof. E. I. Solomon for the use of EPR and UV/Vis/NIR instruments, P. Verma and Dr. S. Gorelsky for helpful DFT discussions, and Prof. R. Mukherjee for X-ray analysis.

Supporting information for this article is available on the WWW under http://www.angewandte.org or from the author.

Although extensive spectroscopic and electrochemical data exists for such oxidized complexes, structural data is lacking. Herein we report the X-ray crystal structure of a Ni^{II}–ligand-radical complex ($\mathbf{1}^+$), which has a contracted coordination sphere relative to its neutral analogue **1**. The difference between the first two oxidation waves in the cyclic voltammogram of **1** ($\Delta E = 500$ mV) and those of the Cu ($\Delta E = 205$ mV) and Zn ($\Delta E = 175$ mV) analogues[11] indicates that $\mathbf{1}^+$ is the most delocalized of the series.[12] Interestingly, $\mathbf{1}^+$ is the only derivative that is unable to oxidize benzyl alcohol to benzaldehyde. A highly delocalized structure for $\mathbf{1}^+$ is further supported by the presence of an intense low-energy absorption band at 4700 cm^{-1}, which suggests that $\mathbf{1}^+$ is best described as a class III mixed-valence compound.[12] The improved oxidation method reported herein allows the structural changes upon oxidation to be investigated and the valence tautomerism to be clarified.

Treatment of complex **1** with 1 equivalent of the oxidants $AgSbF_6$ ($E_{1/2} = +650$ mV vs. Fc/Fc^+; Fc: ferrocene) or the thianthrenyl radical $[thianthrene]^{+\bullet}SbF_6^-$ [13] ($E_{1/2} = +890$ mV vs. Fc/Fc^+) in CH_2Cl_2 results in an immediate color change from brown to green, which signifies formation of the $\mathbf{1}^+$ ion. Solutions of the oxidized complex in CH_2Cl_2 are stable for weeks at room temperature in the absence of H_2O. The quick decomposition reported by others[8,9] may be due to the $(NH_4)_2Ce(NO_3)_6$ oxidant, as the Cu analogue of $\mathbf{1}^+$ decomposes rapidly in the presence of nitrate.[11] The improved stability of $\mathbf{1}^+$ under the oxidation conditions reported herein allows the isolation of single crystals of $\mathbf{1}^+$-SbF_6^- suitable for X-ray structural analysis (Figure 1).[14] Limited structural data exists for phenoxyl radical complexes (Cr^{III},[15] Cu^{II},[16] and Zn^{II} [17]), and this is the first structural characterization of a Ni^{II}–phenoxyl complex.

The structures of both **1** and $\mathbf{1}^+$ possess a slightly distorted square-planar geometry about the nickel center with an angle between the N(1)-Ni(1)-O(1) and N(2)-Ni(1)-O(2) planes of 7.6° and 8.6°, respectively. Interestingly, the Ni coordination sphere of $\mathbf{1}^+$ is contracted relative to that of **1** (Table 1).[9] On average, the Ni–O and Ni–N bond lengths both decrease by approximately 0.02 Å in the oxidized complex, which is opposite to that reported for other structurally characterized metal–phenoxyl radical complexes.[15–17] In these complexes, the metal–phenoxyl radical bond lengthens, which is consistent with a decrease of the electron-donating ability of the phenoxyl ligand relative to that of phenolate.

The nearly twofold symmetric structure of $\mathbf{1}^+$ suggests that the oxidation is either delocalized over the whole molecule or localized on the metal.[18] Previous studies on $\mathbf{1}^+$ suggest ligand-based oxidation at all temperatures in the solid state,[8] whereas in solution the locus of oxidation shifts to the metal

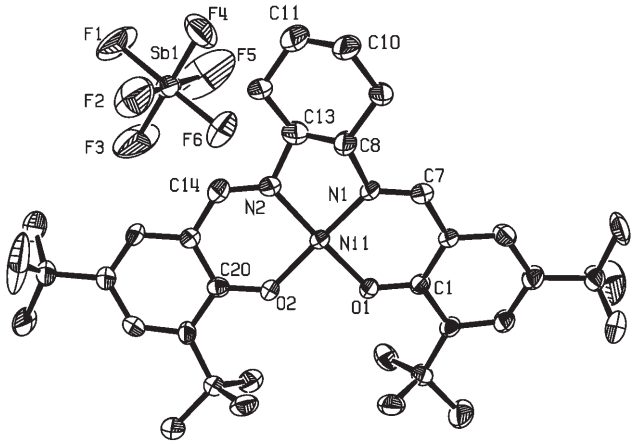

Figure 1. Molecular structure of $\mathbf{1}^{+}$-SbF_6^-. Selected bond lengths [Å] and angles [°]: Ni1–N1 1.825(4), Ni1–N2 1.843(4), Ni1–O1 1.827(3), Ni1–O2 1.830(4), C1–O1 1.299(6), C20–O2 1.302(6), N1–C7 1.304(7), N2–C14 1.293(7), C8–C13 1.450(9), C10–C11 1.442(9); N1-Ni1-N2 85.9(2), O1-Ni1-O2 86.2(2), N1-Ni1-O1 94.2(2), N2-Ni1-O2 94.5(2).

Table 1: Comparsion of experimental and calculated coordination-sphere bond lengths [Å] for **1** and $\mathbf{1}^{+}$.

Bond	**1**[a]	**1**[b] (calcd)	$\mathbf{1}^{+}$	$\mathbf{1}^{+}$[b] (calcd)
Ni1–O1	1.856	1.847	1.827(3)	1.825
Ni1–O2			1.830(4)	
Ni1–N1	1.861	1.841	1.825(4)	1.834
Ni1–N2			1.843(4)	

[a] Average of the two molecules in the unit cell. [b] Computational values for **1** and $\mathbf{1}^{+}$ (see the Supporting Information).

at temperatures below 170 K.[8,9] The large difference in the first two oxidation waves for **1** ($\Delta E = 500$ mV), which is attributed to ligand-based oxidation, indicates significant coupling between the two phenolates and points towards a delocalized system in $\mathbf{1}^{+}$.[12] Delocalization of the ligand radical in solution is further supported by comparative Raman studies on **1** and $\mathbf{1}^{+}$ which suggest a symmetric oxidized structure.[8]

DFT calculations on **1** and $\mathbf{1}^{+}$ consistently reproduce the experimentally observed contraction of the coordination sphere upon oxidation (Table 1). Oxidation of **1** to $\mathbf{1}^{+}$ occurs through removal of an electron from a predominantly ligand-based π* orbital; the HOMO of **1** is effectively the LUMO of $\mathbf{1}^{+}$ (Figure S1 in the Supporting Information). Further analysis shows that removal of an electron from a primarily ligand-based antibonding orbital results in contraction of the coordination sphere, in large part due to increased M→L back-donation. Calculations also support a delocalized ligand-radical electronic structure for $\mathbf{1}^{+}$. The SOMO for $\mathbf{1}^{+}$ (Figure 2) is distributed mainly on the ligand with a 14% contribution from the Ni d_{yz} orbital.[19] The spin density shows a typical pattern for a phenoxyl radical on each ring,[10] with positive spin population at the O (0.16), C_{ortho} (0.10, 0.09), and C_{para} (0.15) positions, accounting for 81% of the total spin density (Figure S2 in the Supporting Information). However, the X-ray structure of $\mathbf{1}^{+}$ does not display a typical quinoid

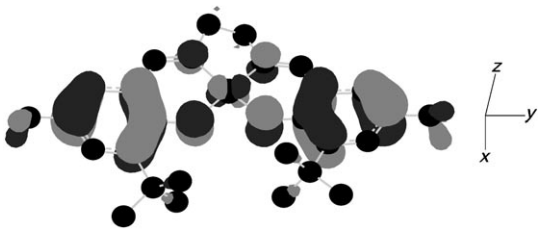

Figure 2. Singly occupied molecular orbital (SOMO) of $\mathbf{1}^{+}$ showing the 14% contribution of the Ni d_{yz} orbital.

bonding pattern, likely because of delocalization of the radical over both ring systems.

Ni L-edge X-ray absorption spectroscopy is a direct probe of the charge and ligand field of the Ni center in the complex and assesses the relative oxidation level of the Ni center.[20] The normalized L-edge spectra of **1** and $\mathbf{1}^{+}$ (Figure S3 in the Supporting Information) are within the expected range for Ni^{II} compounds.[21] The similarity between the energies of the L_3 edges for **1** (854.1 eV) and $\mathbf{1}^{+}$ (854.4 eV) indicates that the Ni oxidation state remains as Ni^{II} in the one-electron-oxidized complex.[22]

The EPR spectrum of $\mathbf{1}^{+}$ in CH_2Cl_2 in the temperature range 5–295 K exhibits a broad ($S = 1/2$) signal at $g_{iso} = 2.045$ (Figure 3a), which indicates that the unpaired electron is

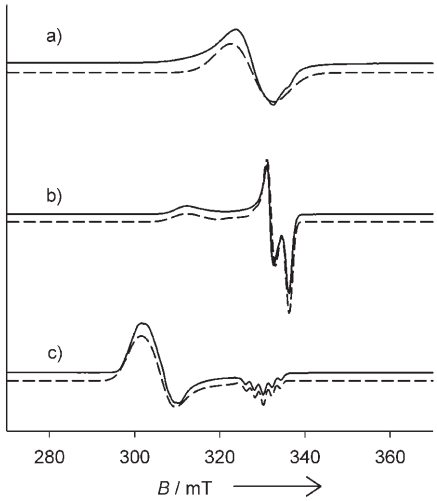

Figure 3. X-band EPR spectra of $\mathbf{1}^{+}$ recorded in frozen CH_2Cl_2 at 77 K (experimental spectra: solid lines; simulations: dashed lines): a) 1 mM $\mathbf{1}^{+}$, b) 1 mM $\mathbf{1}^{+}$ + 0.1 M TBAP, c) 1 mM $\mathbf{1}^{+}$ + 2 equiv pyridine.

predominantly ligand-based. This g value is intermediate between that for the Zn analogue of $\mathbf{1}^{+}$ ($g_{iso} = 2.005$), which is typical for a coordinated phenoxyl radical, and that typical of a Ni^{III} complex ($g_{av} = 2.13$–2.17).[23] The shifting of the signal away from the free-electron value is in agreement with the nonnegligible contribution of the metal d orbitals to the SOMO of $\mathbf{1}^{+}$. The observation of an isotropic signal for $\mathbf{1}^{+}$, regardless of temperature, contrasts with the temperature-dependent valence tautomerism $[Ni^{II}–{}^{\cdot}OPh] \leftrightarrow [Ni^{III}–{}^{-}OPh]$

reported for the identical complex by Shimazaki et al.[9] The discrepancy is attributable to the different oxidation procedures, and more specifically the use of nonligating counterions (SbF_6^- or BF_4^-) in this work. Temperature-dependent valence tautomerism has also been reported for $\mathbf{2}^+$[7,8] and $\mathbf{3}^+$,[6] whereas the analogous complex $\mathbf{4}^+$[10] was found to be a ligand radical in the range 10–295 K. Recent reports have suggested that these tautomeric shifts are associated with axial binding of water or other impurities at the solvent freezing point, rather than a shift in the locus of oxidation due to temperature alone.[8,10]

In an effort to understand this process further, a solution of $\mathbf{1}^+$ in the presence of a 100-fold excess of tetrabutylammonium perchlorate (TBAP) was studied by EPR spectroscopy (Figure 3b). A rhombic signal was observed at 77 K ($g_{11}=2.15$; $g_{22}=2.02$; $g_{33}=1.99$; $g_{av}=2.05$), analogous to $\mathbf{4}^+$ under similar conditions.[10] Although different from that in the EPR spectrum of $\mathbf{1}^+$ in the absence of supporting electrolyte, the g_{av} value indicates that $\mathbf{1}^+$ remains a ligand radical under these conditions. The resolution of a rhombic spin pattern for $\mathbf{1}^+$ is presumably due to more efficient electronic isolation in the presence of excess supporting electrolyte. Interestingly, the addition of approximately 3 equivalents of tetrabutylammonium nitrate to a solution of $\mathbf{1}^+$ at 230 K and subsequent cooling to 77 K results in a rhombic EPR pattern that is consistent with the formation of a Ni^{III} species ($g_x=2.305$; $g_y=2.235$; $g_z=2.015$; $g_{av}=2.19$). This result suggests that modulation of the ligand field by axial binding of nitrate upon cooling, rather than temperature variation alone,[8,9] induces the reported valence tautomerism for $\mathbf{1}^+$. The expected increase in affinity for axial ligands at lower temperatures is known for similar square-planar Ni complexes.[5,6]

Addition of excess pyridine to a solution of $\mathbf{1}^+$ in CH_2Cl_2 results in an immediate color change to red and the appearance of a rhombic EPR pattern ($g_x=2.230$; $g_y=2.185$; $g_z=2.028$, $A_z=20\times10^{-4}\,cm^{-1}$; $g_{av}=2.15$) characteristic of a low-spin Ni^{III} complex with a d_{z^2} electronic ground state (Figure 3c). The five-line superhyperfine pattern in the high-field component is assigned to two equivalent pyridine ligands axially bound to the Ni^{III} center to form $\mathbf{1}$-py_2^+. Similarly to the findings of others,[6,7] axial coordination of pyridine to $\mathbf{1}^+$ shifts the d_{z^2} orbital to higher energy, resulting in the transfer of an electron from the metal center to the ligand. Computational studies on $\mathbf{1}$-py_2^+ (Figure S4 in the Supporting Information) demonstrate an increase in spin density on Ni from 0.15 (for $\mathbf{1}^+$) to 0.93, which is consistent with this shift in the locus of oxidation.

The electronic spectrum of $\mathbf{1}$ (Figure 4, Table 2) is typical of a low-spin d^8 square-planar Ni^{II} complex[7,10] and changes substantially upon oxidation to $\mathbf{1}^+$, particularly in the low-energy region. Low-energy absorption bands for $\mathbf{1}^+$ appear at 11300 and 9200 cm^{-1}, as previously reported by Shimazaki et al.,[9] and similar transitions are reported for $\mathbf{2}^+$, $\mathbf{3}^+$, and $\mathbf{4}^+$.[6–8,10] Interestingly, $\mathbf{1}^+$ exhibits an intense NIR band at 4700 cm^{-1} ($\varepsilon=21500\,M^{-1}cm^{-1}$). Analysis of the shape and intensity of the band,[24] coupled with the extensive delocalization predicted by calculations, allows the assignment of $\mathbf{1}^+$ as a class III mixed-valence complex.[12,25] The class II/class III description for the Cu analogue of $\mathbf{1}^+$[26] accounts for the lower intensity of the corresponding NIR band in this derivative.[11] Changing the metal ion bridge (Cu to Ni) between the mixed-valence ligands affects the degree of delocalization in the oxidized derivatives, which is manifested in the shape and intensity of the corresponding NIR bands. The absence of intense low-energy absorptions in the electronic spectra of $\mathbf{1}$ and $\mathbf{1}$-py_2^+ indicates that the transitions for $\mathbf{1}^+$ in this region are associated with the ligand radical.

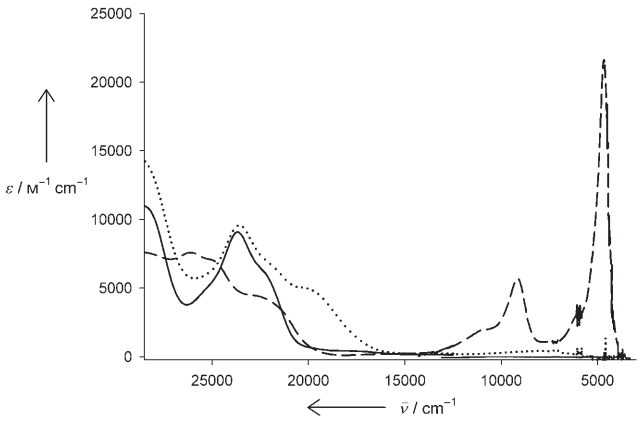

Figure 4. Electronic spectra of 0.08 mM solutions of $\mathbf{1}$ (solid line) and $\mathbf{1}^+$ (dashed line) in CH_2Cl_2, and $\mathbf{1}$-py_2^+ (dotted line) in 1:1 CH_2Cl_2/pyridine.

Table 2: Electronic absorption properties.

Complex	$\bar{\nu}_{max}$ [cm^{-1}] (ε [$10^3\,M^{-1}cm^{-1}$])[c]
$\mathbf{1}$[a]	23700 (9.1), 22500 sh (6.5), 18000 br (0.4)
$\mathbf{1}^+$[a]	26000 (7.6), 25000 sh (7.0), 22000 (4.0), 11300 (1.7), 9200 (5.7), 4700 (21.5)
$\mathbf{1}$-py_2^+[b]	23600 (9.5), 22000 sh (6.8), 20000 (4.9), 7900 br (0.4)

[a] In CH_2Cl_2; [b] in 1:1 CH_2Cl_2/pyridine; [c] sh: shoulder, br: broad.

Time-dependent DFT calculations[27] predicts correctly the absence of intense transitions for $\mathbf{1}$ and $\mathbf{1}$-py_2^+ at energies lower than 18000 cm^{-1} and the existence of two low-energy transitions at 11000 ($f=0.058$) and 5900 cm^{-1} ($f=0.181$) for $\mathbf{1}^+$. These absorptions are blue-shifted slightly relative to the experimental spectra, but have the correct intensity ratio. Of particular interest is the nature of the intense NIR transition of $\mathbf{1}^+$. The principal calculated electronic excitation (74%) that contributes to this intense low-energy absorption is a βHOMO→βLUMO transition (Figure S1 in the Supporting Information). Both the donor and acceptor orbitals are delocalized π orbitals primarily based on the ligand, supporting the conclusion that the low-energy absorption bands for $\mathbf{1}^+$ are delocalized ligand-radical transitions.

In summary, we present the X-ray structure of a Ni^{II}–salen ligand-radical complex, which exhibits a contracted coordination sphere relative to the unoxidized form. The intense low-energy absorption of $\mathbf{1}^+$ is best described as a ligand-radical transition of a highly delocalized class III mixed-valence compound.

Experimental Section

Compound **1**,[28] its Zn analogue,[29] and [thianthrene]$^{+\cdot}SbF_6^{-}$[13] were synthesized by reported methods. $\mathbf{1}^+$ was synthesized by the addition of one equivalent of either [thianthrene]$^{+\cdot}SbF_6^-$ or $AgSbF_6$ to a solution of **1** in CH_2Cl_2. Elemental analysis calcd (%) for $C_{32}H_{52}N_2O_2NiSbF_6$: C 51.52, H 6.24, N 3.34; found: C 51.26, H 5.91, N 3.21. Experimental, instrument, and computational details are presented in the Supporting Information.

Received: March 18, 2007
Revised: April 27, 2007
Published online: June 1, 2007

Keywords: electronic structure · mixed-valent compounds · N,O ligands · nickel · oxidation

[1] a) J. Stubbe, W. A. van der Donk, *Chem. Rev.* **1998**, *98*, 705; b) J. W. Whittaker, *Chem. Rev.* **2003**, *103*, 2347.
[2] H. Ohtsu, K. Tanaka, *Angew. Chem.* **2004**, *116*, 6461; *Angew. Chem. Int. Ed.* **2004**, *43*, 6301.
[3] a) C. G. Pierpont, *Coord. Chem. Rev.* **2001**, *216*, 99; b) P. Ghosh, A. Begum, D. Herebian, E. Bothe, K. Hildenbrand, T. Weyhermuller, K. Wieghardt, *Angew. Chem.* **2003**, *115*, 581; *Angew. Chem. Int. Ed.* **2003**, *42*, 563; c) P. Chaudhuri, K. Wieghardt, *Prog. Inorg. Chem.* **2001**, *50*, 151; d) R. H. Felton, in *The Porphyrins*, *Vol. V* (Ed.: D. Dolphin), Academic, New York, **1978**, p. 53.
[4] D. Dolphin, T. Niem, R. H. Felton, I. Fujita, *J. Am. Chem. Soc.* **1975**, *97*, 5288.
[5] H. Ohtsu, K. Tanaka, *Inorg. Chem.* **2004**, *43*, 3024.
[6] O. Rotthaus, O. Jarjayes, F. Thomas, C. Philouze, C. Perez Del Valle, E. Saint-Aman, J. L. Pierre, *Chem. Eur. J.* **2006**, *12*, 2293.
[7] O. Rotthaus, F. Thomas, O. Jarjayes, C. Philouze, E. Saint-Aman, J. L. Pierre, *Chem. Eur. J.* **2006**, *12*, 6953.
[8] Y. Shimazaki, T. Yajima, F. Tani, S. Karasawa, K. Fukui, Y. Naruta, O. Yamauchi, *J. Am. Chem. Soc.* **2007**, *129*, 2559.
[9] Y. Shimazaki, F. Tani, K. Fukui, Y. Naruta, O. Yamauchi, *J. Am. Chem. Soc.* **2003**, *125*, 10512.
[10] L. Benisvy, R. Kannappan, Y. F. Song, S. Milikisyants, M. Huber, I. Mutikainen, U. Turpeinen, P. Garnez, L. Bernasconi, E. J. Baerends, F. Hartl, J. Reedijk, *Eur. J. Inorg. Chem.* **2007**, 631.
[11] R. C. Pratt, T. D. P. Stack, *J. Am. Chem. Soc.* **2003**, *125*, 8716. See the Supporting Information for further details.
[12] D. M. D'Alessandro, F. R. Keene, *Chem. Soc. Rev.* **2006**, *35*, 424.
[13] N. G. Connelly, W. E. Geiger, *Chem. Rev.* **1996**, *96*, 877.
[14] See the Supporting Information for details of the X-ray analysis. CCDC-637662 contains the supplementary crystallographic data for this paper. These data can be obtained free of charge from The Cambridge Crystallographic Data Centre via www.ccdc.cam.ac.uk/data_request/cif.
[15] A. Sokolowski, E. Bothe, E. Bill, T. Weyhermuller, K. Wieghardt, *Chem. Commun.* **1996**, 1671.
[16] L. Benisvy, A. J. Blake, D. Collison, E. S. Davies, C. D. Garner, E. J. L. McInnes, J. McMaster, G. Whittaker, C. Wilson, *Chem. Commun.* **2001**, 1824.
[17] L. Benisvy, A. J. Blake, D. Collison, E. S. Davies, C. D. Garner, E. J. L. McInnes, J. McMaster, G. Whittaker, C. Wilson, *Dalton Trans.* **2003**, 1975.
[18] Structural characterization of the Ni^{II} and Ni^{III} complexes of a $N_2S_2^{4-}$ ligand shows a contraction of the coordination sphere upon oxidation. J. Hanss, H. J. Krüger, *Angew. Chem.* **1998**, *110*, 366; *Angew. Chem. Int. Ed.* **1998**, *37*, 360.
[19] S. I. Gorelsky, *AOMIX*, Department of Chemistry, York University, Toronto, Canada (http://sg-chem.net).
[20] A solid sample of $\mathbf{1}^+$-BF_4^- was synthesized for the L-edge experiments because of concerns of interference from Sb absorptions.
[21] C. Y. Ralston, H. X. Wang, S. W. Ragsdale, M. Kumar, N. J. Spangler, P. W. Ludden, W. Gu, R. M. Jones, D. S. Patil, S. P. Cramer, *J. Am. Chem. Soc.* **2000**, *122*, 10553.
[22] R. Sarangi, S. D. George, D. J. Rudd, R. K. Szilagyi, X. Ribas, C. Rovira, M. Almeida, K. O. Hodgson, B. Hedman, E. I. Solomon, *J. Am. Chem. Soc.* **2007**, *129*, 2316.
[23] a) X. Ottenwaelder, R. Ruiz-Garcia, G. Blondin, R. Carasco, J. Cano, D. Lexa, Y. Journaux, A. Aukauloo, *Chem. Commun.* **2004**, 504, and references therein; b) R. S. Drago, E. I. Baucom, *Inorg. Chem.* **1972**, *11*, 2064; c) H. J. Krüger, R. H. Holm, *Inorg. Chem.* **1987**, *26*, 3645.
[24] The intense transition is essentially solvent-independent ($\nu_{max} = 4750\ cm^{-1}$ in CH_3CN) with a narrow bandwidth ($\Delta\nu_{1/2} = 670\ cm^{-1}$). The calculated $\Delta\nu_{1/2}$ is 20% of the predicted minimum bandwidth in the high-temperature limit ($\Delta\nu_{HTL} = \sqrt{16 \ln 2\, R T \nu_{max}} = 3300\ cm^{-1}$), which is consistent with the inability of Marcus–Hush theory to predict IVCT band shape at the class II/III borderline.[28] Furthermore, the band at $4700\ cm^{-1}$ is asymmetric, which provides further support that $\mathbf{1}^+$ is a borderline class II/III or class III mixed-valence complex.
[25] S. F. Nelsen, *Chem. Eur. J.* **2000**, *6*, 581.
[26] R. C. Pratt, T. Storr, T. D. P. Stack, unpublished results.
[27] a) M. E. Casida in *Recent Advances in Density Functional Methods* (Ed.: D. P. Chong), World Scientific, Singapore, **1995**, p. 155; b) R. E. Stratmann, G. E. Scuseria, M. J. Frisch, *J. Chem. Phys.* **1998**, *109*, 8218.
[28] W. H. Leung, E. Y. Y. Chan, E. K. F. Chow, I. D. Williams, S. M. Peng, *J. Chem. Soc. Dalton Trans.* **1996**, 1229.
[29] G. A. Morris, H. Y. Zhou, C. L. Stern, S. T. Nguyen, *Inorg. Chem.* **2001**, *40*, 3222.

